Scientific Research Publishing

Journal of Applied Mathematics and Physics, 2022, 10, 1887-1897
https://www.scirp.org/journal/jamp
ISSN Online: 2327-4379
ISSN Print: 2327-4352

Signs of Phase Transition in High Energy Proton-Proton Collisions

Mohamed Tarek Hussein*, Mohamed Tawfik Ghoneim, Zeinab Abdel-Halim

Faculty of Science, Cairo University, Cairo, Egypt
Email: *tarek@sci.cu.edu.eg, ghoneim@sci.cu.edu.eg, zabdelhalim@sci.cu.edu.eg

How to cite this paper: Hussein, M.T., Ghoneim, M.T. and Abdel-Halim, Z.A. (2022) Signs of Phase Transition in High Energy Proton-Proton Collisions. *Journal of Applied Mathematics and Physics*, **10**, 1887-1897.
https://doi.org/10.4236/jamp.2022.106129

Received: May 12, 2022
Accepted: June 21, 2022
Published: June 24, 2022

Abstract

The present work aims to study the possible states of matter and the location of phase boundaries between hadronic gas and the quark-gluon plasma QGP. The boundary at the hadron freeze-out is also considered. Proton-proton collisions at a wide range of center of mass energies are used to examine the phase transition (entropy-temperature) diagram. Local thermodynamic equilibrium is assumed at different intervals of rapidity space. The entropy of the system is expressed in terms of the multiplicity of hadron production in each interval. However, the local temperature is estimated using the average transverse momentum. The values of the critical temperatures are found at the boundaries of the phases with a quite clear description of the states.

Keywords

Proton-Proton Collision, Quark-Gluon Plasma (QGP), Phase Transition, Quantum Chromo Dynamics (QCD)

1. Introduction

The quantum chromodynamics (QCD) phase diagram [1] contains a variety of theoretically predicted features. The most important one is the phase boundary which separates the hadron gas phase and the quark-gluon plasma phase. We are going to collect information on the properties of the QCD phase diagram through systematic studies of the system size and the energy dependence of particle production in hadron-hadron collisions at a wide range of interaction energy.

Generally, the phase transition can be examined by following changes in temperature, pressure, entropy… etc. of the system. So, when the nuclear matter goes through high energy collisions creates high temperatures and high densities like that of the core of the sun (5 - 10 times the density of nuclear matter) [2].

These conditions force the nuclear matter to go through a phase transition and get into the quark-gluon plasma (QGP) phase which still has a mysterious nature. After the expansion of the system, this hot de-confinement state QGP goes through a phase of forming a large number of hadron particles. The high multiplicity of the produced hadron particles generated by the same scenario through the proton-proton collision experiments could be handled by thermal-statistical models. Once the system reaches near thermal equilibrium, one can extract its characteristics by several thermo-dynamical observables such as its volume, temperature, energy density and entropy.

While the order of phase transition will be viewed in the frame of the thermodynamic picture the nature of transition can be a genuine phase transition, first-order or crossover over a small temperature range. The first-order phase transition is characterized by continuous behavior; however, the crossover is a rapid change with temperature.

The particle production through the proton-proton collisions will be considered the key player in detecting the phase transition and getting a sufficient view of the nature of the strong force acting inside the hadron and studying its dependence on the number of quarks flavors and colors.

The predictions on the location of the critical temperature at which phase transition turns on are still very uncertain. Recently found, that the phase diagram might contain yet another phase, the so-called quarkyonic phase [3] [4], which would be separated from normal hadronic matter by a different phase boundary line.

Experimentally, there are several control parameters available that might allow studying different regions of the phase diagram with hadron collisions. One is the variation of the center-of-mass energy which will force the reaction systems to follow different trajectories in the temperature-chemical potential (T-μ plane), reflected by a change in the chemical freeze-out parameters. The second control parameter is the variation of the system size, which can either be achieved by performing collisions of hadrons (at different impact parameters) of different sizes; or by studying centrality selected minimum bias collisions considering the entropy density versus temperature at different rapidity intervals. This can be considered a good control parameter for probing different areas of the phase diagram and shall be discussed further below.

In order to determine different areas in the QCD phase diagram, the variation of the center-of-mass energy can be considered the best-defined control parameter. In an energy range starting from a few GeV up to the TeV region, a wide region in the entropy-temperature (σ-T) plane can be explored experimentally, as is evident from the strong dependence of the temperature freeze-out parameters on the energy. It is unlikely to consider the freeze-out temperatures of the overlap interacting part (fireball) vary with their size. The trajectories of the fireballs in the core might be always the same, irrespective of their size [5]. So, studying centrality dependences in asymmetric proton-hadron reaction systems could provide an additional experimental test of the production mechanism [6].

In this article, we study the experimental features which point out the existence of the phase transition and its nature by relating the change in the macroscopic variables such as transverse momentum, and multiplicity distribution to the microscopic hypothesis of the transition mechanism.

The paper is organized as follows:

Section 1 is the Introduction

Section 2 is Particle Production Mechanism

Section 3 is Results and Discussion

Section 4 is Conclusive Remarks

Finally, references come at the end of the article.

2. Particle Production Mechanism

Particle production is an important feature that provides statistical models with the appropriate data for describing thermodynamic phenomena. These models are based on the assumption that the particle yields correspond to their thermal equilibrium or local equilibrium, and can thus be described by the parameters; temperature T, chemical potential μ, entropy σ, and the interaction volume V. In the following we shall consider two scenarios in describing the particle production. In a macroscopic model, the production of particles through fireball formation is reasonable to give an overview of the thermodynamic formation of the system. On the other hand, a microscopic model gives more details about the quark structure of the interacting hadrons and produces jets through string formation.

The colliding nucleons may emerge as drops containing some kind of mesonic matter. These drops are called "fireballs". The principle of fireball is considered with the goal to detect the QCD critical point and first-order phase transition. Interpreting these experimental signals requires a deep understanding of the critical phenomena and the non-equilibrium dynamics of the rapidly expanding fireball. We shall use the multi-string fragmentation mechanism [6] [7] to describe the particle production in hadron-hadron collision. It is assumed that pp interactions go through binary collisions between their constituent quarks. The number of quark pairs contributing to the reaction depends mainly on the impact parameter according to geometrical aspects. The range of impact parameters is divided into three regions. 1) The most peripheral region where only one pair of interacting quarks exists. 2) The intermediate region where two quark pairs are considered. 3) The region of the central collision, where all constituent quarks may contribute to the reaction. Each region is defined by specific limits of the impact parameter "b" and the weight factor for each is determined by the area of the overlap region.

$$P(v) = \int_{L(v)}^{U(v)} 2\pi b \mathrm{d}b \tag{1}$$

where $L(v)$ and $U(v)$ are the lower and the upper limits of the region, respectively and v indicates the number of quark pairs which may participate in the colli-

sion. The relation between b and v is calculated according to a geometrical picture where each colliding particle makes a cylindrical cut in the other. The total interaction energy is distributed among the possible pairs. Each quark pair may form a string according to the string dynamics [6] which consider that a string can be formed due to the color field existing between two interacting quarks. Hadrons are formed in two jet structure events by the successive fragmentation of the string. Let us consider a jet formed by an original quark q_0 with energy ϵ_0. At the first vertex of fragmentation, the string breaks up producing quark-quark qq with energy $z\epsilon_0$ leaving the string with residual energy $\epsilon_1 = (1 - z)\epsilon_0$, where z is a fraction $0 < z < 1$ and has a certain distribution $f(z)$. Further fragmentation of the string will produce $q\bar{q}$ pairs in rank order forming mesons, whose i^{th} rank order has energy $z\epsilon_{i-1}$. The length of the string depends mainly on the original quark energy ϵ_0 and the fragmentation function $f(z)$. The multiple breaks of strings increase the number of created point-like particles (quarks and gluons) consequently, increase the entropy of the system and could refer to the boundary of the phases. A long string has a large number of vertices and in turn a high multiplicity of produced mesons.

3. Results and Discussion

We build up our study on the measurements from certain experimental collaborations such as the private communication with the CERN library through the particle data group PDG and HEPData [8]. We are particularly concerned about the transverse momentum spectra of produced hadron particles at different centre mass of energy which has arranged in the format of the multiplicity distribution through the transverse momentum and rapidity intervals $\frac{\mathrm{d}^2 N}{\mathrm{d}p_t \mathrm{d}y}$ versus the transverse momentum p_t of the produced hadrons out coming from the inelastic proton-proton collision at the centre of mass energies $\sqrt{s} = 6.3, 7.7, 8.8, 12.3, 17.3\ \text{GeV}$ which was carried out at the CERN Super Proton Synchrotron by the multi-purpose NA61/SHINE [9]. For covering a large band of the interaction energy in the region we applied the same process to the produced particles from the p-p interactions at the centre of mass energies $\sqrt{s} = 0.9, 2.36, 7.0\ \text{TeV}$ which were measured using the inner tracking CMS (compact muon solenoid) experiment at LHC [10] [11], through which detecting product of collisions between protons travelling by speed nearly the speed of light. At the centre of this detector where the particles collide there is recreating the same conditions from temperature and density aspects of the early universe as expected after a long time since the big bang.

In the beginning, the transverse momentum distributions of produced pions in pp collisions at $\sqrt{s} = 6.3\ \text{GeV}$ (as an example of ISR energy) are studied for each interval in the whole rapidity range as given in **Figure 1**. It is found that all the data in **Figure 1** could be fitted by the modified Boltzmann distribution. This means that in each rapidity interval, the particles are produced in local

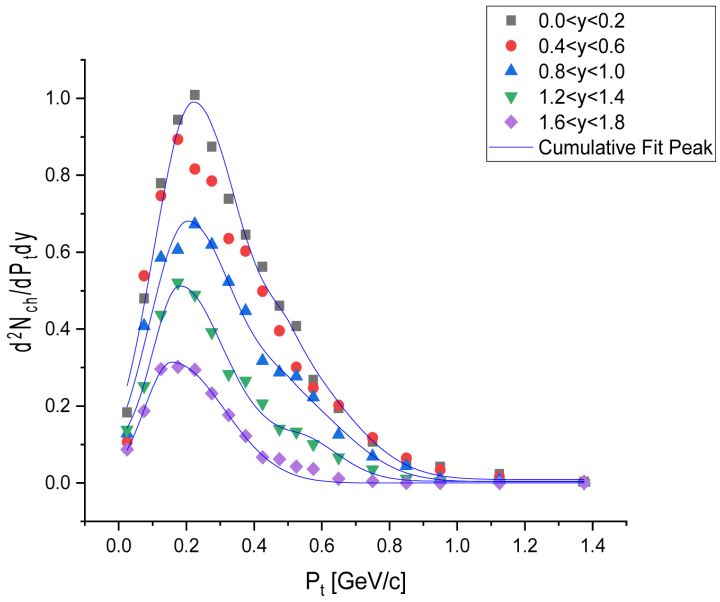

Figure 1. Transverse momentum of pions produced in pp collisions at $\sqrt{s} = 6.3\,\text{GeV}$ for different rapidity intervals. The solid lines are the fitting lines by the Boltzmann distribution.

equilibrium and the temperature is determined by thermodynamic tools using Mathematica software.

In order to construct the phase diagram, we have to define some important thermodynamic parameters, such as the energy density based on the thermal-statistical model and using macroscopic observables such as the volume, the multiplicity distribution and the transverse momentum. We could deduce the initial energy density in the system of a head-on collision given by [12],

$$\varepsilon = \frac{3}{2}\langle p_t \rangle \frac{\mathrm{d}N/\mathrm{d}y}{V} \tag{2}$$

Also, we could estimate the initial entropy density in the system of a head-on collision, given by [13],

$$\sigma = \frac{3}{2}\frac{\mathrm{d}N/\mathrm{d}y}{S} \tag{3}$$

The rapidity density $\mathrm{d}N/\mathrm{d}y$ represents the number of produced pions in the rapidity interval $\mathrm{d}y$ and V and S are the interaction volume and surface area of the overlap region of the two colliding particles that depends mainly on the impact parameter. The values of entropy density vary due to the estimation of the area S. Both the energy density and the random motion increase with the multiplicity per rapidity interval.

The rapidity density σ is a good parameter to form the phase transition diagram (σ-T) and locate the critical point [14]. One also has to find a tool for measuring the temperature at the points of equilibrium of the system under consideration. Simply, the average transverse momentum is calculated at each rapidity interval given in **Figure 1** assuming local equilibrium at each interval. The

transverse momentum P_t distribution is given by [15] [16].

$$f\left(P_t\right)=\frac{1}{P_t}\frac{\mathrm{d}N}{\mathrm{d}P_t}\approx A\exp^{-\frac{P_t}{T_{eff}}} \tag{4}$$

where A is the normalization factor while T_{eff} is the effective local temperature of the system which is smaller than the initial temperature because of the longitudinal cooling [17] [18]. T_{eff} can be estimated using the average value of the transverse momentum for the finite range of P_t as following [17] [18] [19]:

$$\left\langle P_t\right\rangle=\frac{\int_a^b P_t\mathrm{d}P_t P_t f\left(P_t\right)}{\int_a^b \mathrm{d}P_t P_t f\left(P_t\right)} \tag{5}$$

$$\left\langle P_t\right\rangle=2T_{eff}+\frac{a^2\mathrm{e}^{-\frac{a}{T_{eff}}}-b^2\mathrm{e}^{-\frac{b}{T_{eff}}}}{\left(a+T_{eff}\right)\mathrm{e}^{-\frac{a}{T_{eff}}}-\left(b+T_{eff}\right)\mathrm{e}^{-\frac{b}{T_{eff}}}} \tag{6}$$

where a and b are the limits of the transverse momentum P_t in each rapidity interval. The value of T_{eff} is found by the inverse solution of Equation (6). **Table 1** refers to the temperature of the system during the particle emission assuming that each rapidity interval represents a source with local equilibrium.

The first column in **Table 1** represents the value of the mid interval of the rapidity, the second column is the rapidity distribution (the multiplicity in each rapidity interval), the average of transverse momentum $\left\langle P_t\right\rangle$ in the third column is the experimental values of the transverse momentum in the corresponding rapidity interval, and T_{eff} in the last column is the inverse solution Equation (6). It is clear that at central rapidity, the yield of pions is maximum. Also, the temperature decreases gradually from the center toward the peripheral region.

Table 1. The experimental parameters and the effective temperature of produced hadron through proton-proton collision at different rapidity interval.

$\mathrm{pp}\to\pi^-+\mathrm{x}$ $P_{lab}=20\ \mathrm{GeV/c}$, $\sqrt{s_{NN}}=6.3\ \mathrm{GeV}$			
y	$\mathrm{d}N/\mathrm{d}y$	$\left\langle P_t\right\rangle$ "GeV/c"	T_{Eff} "GeV"
0.1	7.78	0.308	0.133
0.3	7.41	0.317	0.137
0.5	7.00	0.307	0.132
0.7	6.30	0.308	0.132
0.9	5.36	0.300	0.128
1.1	4.39	0.289	0.122
1.3	3.48	0.271	0.112
1.5	2.47	0.250	0.100
1.7	1.92	0.234	0.091
1.9	1.29	0.207	0.075

Now we can obtain the relation between the entropy density σ and the temperature T, which seems to resemble the formation of the curves predicted for hadronic matter with crossover to QGP. This relation contains the relevant information, which translates as a phase transition diagram and may serve as a probe for the state of hot hadronic matter and could provide a signal for the de-confinement transition of hadronic matter.

The nature of transition can be a genuine phase transition (first-order or continuous), or just a rapid change (crossover) over a small temperature range. Estimates of energy densities which can be achieved in ultra-relativistic pp collisions with high multiplicities suggest values sufficiently high for experimental formation of the QGP [20] [21] [22].

We considered two ranges of interaction energies. The pp collisions at few GeV are shown in **Figure 2** and the ultra-high-energy collisions at TeV region are given in **Figure 3**.

In detail, **Figure 2** shows that the σ-T relation is mostly independent on the center of mass energy $\sqrt{s}$ within the ISR range. Each point in the graph is a property of the rapidity interval and characterized by its local temperature. The entropy starts increasing gradually with the temperature T with a small slope of about 15.4 $\text{fm}^{-2}\cdot\text{GeV}^{-1}$ (represented by the red line) due to the hadron dissociation forming the hadronic gas. At $T \approx 130$ MeV = T_c (critical temperature), the slope of the curves increases to about 180 $\text{fm}^{-2}\cdot\text{GeV}^{-1}$ (represented by the blue line)

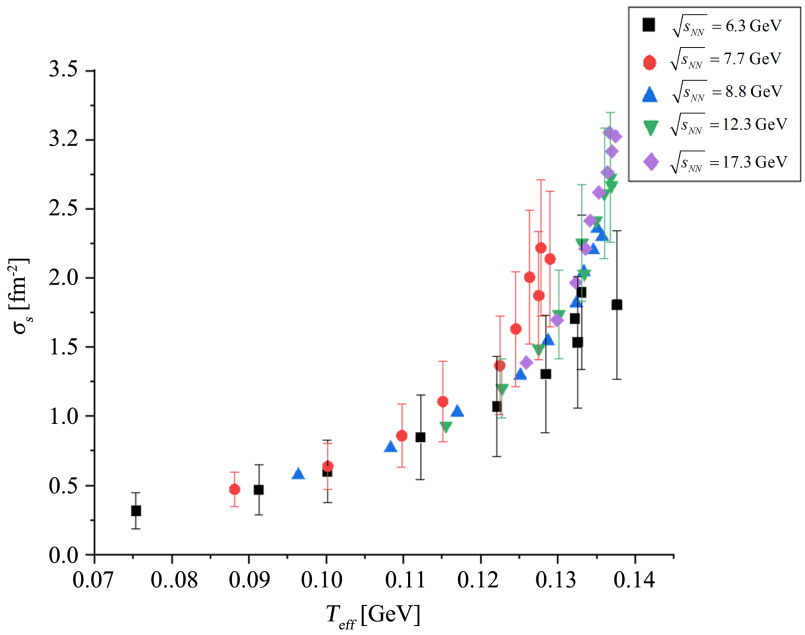

Figure 2. The relation between the entropy σ and the effective temperature T_{eff} of the interacting system produced in pp collisions at 6.3, 7.7, 8.8, 12.3 and 17.3 GeV. The vertical lines correspond to the statistical error bars. The diagram could be divided into two linear regions, the first (red line) has small slop with a gradient ≈ 15.4 $\text{fm}^{-2}\cdot\text{GeV}^{-1}$ describing the hadron dissociation. The second one (blue line) has a bigger gradient ≈ 180 $\text{fm}^{-2}\cdot\text{GeV}^{-1}$ representing the QGP phase. The black arrow refers to the critical temperature T_c = 130 GeV at the boundary of the two phases.

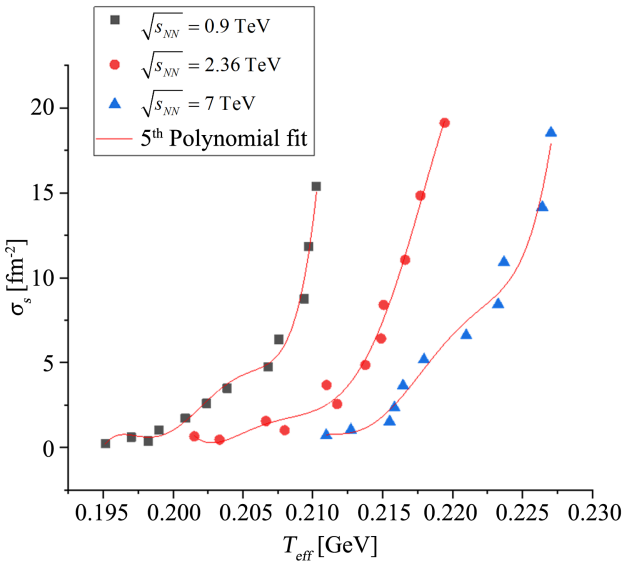

Figure 3. The relation between the entropy σ and the effective temperature T_{eff} of the interacting system produced in pp collisions at 0.90, 2.36 and 7 TeV.

referring to the creation of quark pairs in string form and could be interpreted as a crossover transition to the QGP phase. As the temperature increases again, accordingly σ increases due to the rapidly new created quark pairs.

On the other hand, at the ultra-high-energy we see different phenomena, where the σ-T relation shows a strong dependence on the center of mass energy $\sqrt{s}$, producing separate curves as shown in **Figure 3**. As $\sqrt{s}$ increases, the environment is relevant to expand the interaction volume, pushing more heat and increasing the range of the temperature.

We assume the σ versus T dependence shown in **Figure 3** may go first through the simplified case where, at the initial time, the central blob volume V is almost the same in all collisions giving a finite number of hadronic gas (hadron dissociation). The flattening of the temperature T for increasing the number of hadronic gas starts just before the transition is reached. It will continue until σ grows enough with T to reach T_c (black arrows in **Figure 3** refer to the critical temperature T_c) and the environment is relevant for creating strings of quark pairs. Further growth of pairs, consequently, increases the entropy σ through the transition without appreciable change of T with higher steepness in the σ-T curves. The temperature, therefore, changes slowly, and the transverse expansion effect may even decrease as one goes through the transition (as it requires "latent heat"). Above the transition temperature T_c there will be an increase again with growing the string production, but these variations should now have at most a weak flattening effect on the temperature because most hadrons emerging from the central blob will do so when the quark-gluon plasma is cool enough, at cooling temperature "T_{co}" to hadronize, *i.e.*, at $T \sim T_{co}$. The flattening of the curve is expressed as growth above the standard value T_{co} (pointed by the red arrows in **Figure 3**). Values of T_c and T_{co} are summarized in **Table 2** for the different center of mass energies $\sqrt{s}$.

Table 2. The critical temperature T_c and the cooling temperature of the proton collisions at the TeV region.

Center of mass energy $\sqrt{s}$ "TeV"	Critical Temperature T_c "MeV"	Cooling Temperature T_{co} "MeV"
0.9	197	207
2.36	203	212
7.0	216	224

In a forthcoming article, we shall go into another trend, and assume the particle emission through a non-equilibrium system instead of a local equilibrium point source. Moreover, we will consider a non-vanishing chemical potential μ of the created particles and consequently, consider a μ-T phase diagram.

4. Conclusive Remarks

According to thermodynamic features of the charged hadrons produced through the hadron's collision, we can deduce the following:

- The particle production in pp collision is found a good tool to study the interaction mechanism at a wide range of canter of mass energy starting from ISR (few tens of GeV) to the ultra-high-energy TeV CERN-LHC. Data are collected through the Particle Data Group (PDG).
- The phase transition is studied through the entropy-temperature phase diagram σ-T.
- The temperature is calculated by averaging the transverse momentum at different rapidity intervals, assuming that each interval is a point source with local thermodynamic equilibrium, so we can apply Boltzmann statistics. The entropy σ is proportional to the multiplicity of hadrons produced in each rapidity interval dN/dy.
- The σ-T curves show independent behavior on the center of mass energy at the few GeV range. A crossover transition from hadronic matter to QGP phase is observed at $T \approx 130$ MeV. The new phase is formed by creating $q\bar{q}$ strings with the gluon exchange boson.
- The increase of the created strings is the main reason for increasing the entropy.
- At the ultra-high-energy, we found different phenomena, where the σ-T relation shows a strong dependence on the center of mass energy, producing separate curves.
- The critical temperature T_c for the transition from the gas dissociation state to the quark gulon plasma (QGP) phase changes with the center of mass energy $\sqrt{s}$ as given in Table 2.
- A weak flattening effect on the temperature is observed when most hadrons emerge from the central blob when the quark-gluon plasma is cool enough to hadronize, at temperature T_{co}. These values are also presented in Table 2.

- Using the above technique, we could specify the boundary of phase transition and describe and describe its nature whether a genuine phase transition, (first-order) or crossover over a small temperature range.

In a forthcoming article, we shall consider a hadronic system formed at pre-equilibrium thermodynamic state with a non-vanishing chemical potential μ of the created particles and consequently, consider a μ-T phase diagram.

Conflicts of Interest

The authors declare no conflicts of interest regarding the publication of this paper.

References

[1] HotQCD Collaboration (2019) Chiral Crossover in QCD at Zero and Non-Zero Chemical Potentials. *Physics Letters B*, **795**, 15-21. https://doi.org/10.1016/j.physletb.2019.05.013

[2] Ahmad, M.A. (2017) Some Aspects of Simulations and Modeling in Relativistic Nuclear Collisions (*Astro-Particle Physics*). *International Journal of High Energy Physics*, **4**, 58-64. https://doi.org/10.11648/j.ijhep.20170405.12

[3] McLerran, L. and Pisarski, R.D. (2007) Phases of Dense Quarks at Large N_c. *Nuclear Physics A*, **796**, 83-100. https://doi.org/10.1016/j.nuclphysa.2007.08.013

[4] McLerran, L. and Reddy, S. (2019) Quarkyonic Matter and Neutron Stars. *Physical Review Letters*, **122**, Article ID: 122701. https://doi.org/10.1103/PhysRevLett.122.122701

[5] Daftari, I.K. and Roy, T. (1978) Some Observations on Coplanar Decay of Fireballs at 24 GeV/c Proton-Nucleus Interaction. *Czechoslovak Journal of Physics B*, **28**, 521-528. https://doi.org/10.1007/BF01597201

[6] Hussen, M.T., Rabea, A., El-Naghy, A. and Hassan, N.M. (1995) A String Model for Hadron Interactions at High Energies. *Progress of Theoretical Physics*, **93**, 585-595. https://doi.org/10.1143/ptp/93.3.585

[7] Romatschke, P. (2010) New Developments in Relativistic Viscous Hydrodynamics. *International Journal of Modern Physics E*, **19**, 1-53. https://doi.org/10.1142/S0218301310014613

[8] Particle Data Group (2020) Review of Particle Physics. *Progress of Theoretical and Experimental Physics*, **2020**, 083C01. https://doi.org/10.1093/ptep/ptaa104

[9] Abgrall, N., Andreeva, O., Aduszkiewicz, A., Ali, Y., Anticic, T., Antoniou, N., *et al.* (2014) NA61/SHINE Facility at the CERN SPS: Beams and Detector System. *Journal of Instrumentation*, **9**, P06005. https://doi.org/10.1088/1748-0221/9/06/P06005

[10] Khachatryan, V., Sirunyan, A.M., Tumasyan, A., Adam, W., Bergauer, T., Dragicevic, M., *et al.* (2010) Transverse-Momentum and Pseudorapidity Distributions of Charged Hadrons in pp Collisions at $\sqrt{s}$ = 7TeV. *Physical Review Letters*, **105**, Article ID: 022002. https://doi.org/10.1103/PhysRevLett.105.022002

[11] Khachatryan, V., Sirunyan, A., Tumasyan, A., Adam, W., Bergauer, T., Dragicevic, M., *et al.* (2010) Transverse-Momentum and Pseudorapidity Distributions of Charged Hadrons in PP Collisions at $\sqrt{s}$ = 0.9 and 2.36TeV. *Journal of High Energy Physics*, No. 2, 41.

[12] Li, B.C., Bai, T., Guo, Y.Y. and Liu, F.H. (2017) On J/ψ and γ Transverse Momentum Distributions in High Energy Collisions. *Advances in High Energy Physics*,

2017, Article ID: 9383540. https://doi.org/10.1155/2017/9383540

[13] Sa, B.H., Li, X.M., Hu, S.Y., Li, S.P., Feng, J. and Zhou, D.M. (2007) Specific Heat in Hadronic Matter and in Quark-Gluon Matter. *Physical Review C*, **75**, Article ID: 054912. https://doi.org/10.1103/PhysRevC.75.054912

[14] Van Hove, L. (1982) Multiplicity Dependence of P_t Spectrum as a Possible Signal for a Phase Transition in Hadronic Collisions. *Physics Letters B*, **118**, 138-140. https://doi.org/10.1016/0370-2693(82)90617-7

[15] Bjorken, J.D. (1983) Highly Relativistic Nucleus-Nucleus Collisions: The Central Rapidity Region. *Physical Review D*, **27**, 140-151. https://doi.org/10.1103/PhysRevD.27.140

[16] Redlich, K. and Satz, H. (1986) Critical Behavior Near Deconfinement. *Physical Review D*, **33**, 3747-3752. https://doi.org/10.1103/PhysRevD.33.3747

[17] Gardim, F.G., Giacalone, G., Luzum, M. and Ollitrault, J.Y. (2020) Thermodynamics of Hot Strong-Interaction Matter from Ultra-Relativistic Nuclear Collisions. *Nature Physics*, **16**, 615-619. https://doi.org/10.1038/s41567-020-0846-4

[18] Basu, S., Nandi, B.K., Chatterjee, S., Chatterjee, R. and Nayak, T. (2016) Beam Energy Scan of Specific Heat through Temperature Fluctuations in Heavy Ion Collisions. *Journal of Physics*: *Conference Series*, **668**, Article ID: 012043. https://doi.org/10.1088/1742-6596/668/1/012043

[19] Filinov, V. and Larkin, A. (2019) Momentum Distribution Functions in Quark-Gluon Plasma. *Journal of Applied Mathematics and Physics*, **7**, 1997-2014. https://doi.org/10.4236/jamp.2019.79137

[20] Sawy, F.H., Ghoneim, M.T. and Hussein, M.T. (2015) Dynamic Characteristics of Proton-Proton Collisions. *Journal of Nuclear and Particle Physics*, **5**, 89-92.

[21] Wang, X.N. (2014) What Hard Probes Tell Us about the Quark-Gluon Plasma: Theory. *Nuclear Physics A*, **932**, 1-8. https://doi.org/10.1016/j.nuclphysa.2014.09.065

[22] Ghoneim, M.T., Sawy, F.H. and Hussein, M.T. (2015) Particle Production in Proton-Proton Collisions. *International Journal of Physical Sciences*, **10**, 371-377. https://doi.org/10.5897/IJPS2015.4297